Uniform Micro-Sized α- and β-Si_3N_4 Thin Ribbons Grown by a High-Temperature Thermal-Decomposition/Nitridation Route

Junqing Hu,* Yoshio Bando, Zongwen Liu, Fangfang Xu, Takashi Sekiguchi, and Jinhua Zhan[a]

Abstract: Uniform micro-sized α- and β-Si_3N_4 thin ribbons have been achieved by a high-temperature thermal-decomposition/nitridation route. As-grown ribbons were characterized by using powder X-ray diffraction, scanning electron microscopy, transmission electron microscopy, energy-dispersive X-ray spectroscopy, electron energy loss spectroscopy, and cathodoluminescence. These α- and β-Si_3N_4 ribbons are structurally uniform micro-sized single crystals, and have a width of ~2–3 microns, a thickness of ~20–60 nm, and a length, that ranges from several hundreds of microns to the order of millimeters. A room-temperature cathodoluminescence spectrum recorded from these ribbons shows one intensive blue emission peak at ~433 nm. The growth for the new ribbon form of this material is believed to be dominated by a vapor–solid process.

Keywords: crystal growth · nitrides · ribbons · scanning probe microscopy · silicon

Introduction

Inorganic whiskers or fibers have been widely employed to improve toughness in advanced ceramics.[1,2] The use of silicon-nitride polycrystalline fibers and whiskers as a reinforcement in metal-matrix composites (so-called MMCs) is of great interest due to to their outstanding mechanical properties (such as, high strength, high tensility), and their thermal and chemical stability (high resistance to thermal shock and oxidation).[3–8] On the other hand, due to its high dopant concentration similar to the III-N compounds (GaN and AlN), the dopant containing silicon nitride (thin films or large single-crystals) compounds are extensively used in the microelectronics industry for various applications as optical devices, such as a dopant diffusion barriers, an encapsulant for III-V semiconductors, and an interlevel dielectric.[9–11]Silicon nitride (Si_3N_4) usually exists in two structural modifications, namely, α-Si_3N_4 (trigonal, space group: $P31c$) and β-Si_3N_4 (hexagonal, space group: $P6_3/m$). α-Si_3N_4 is regarded as a metastable, low-temperature phase that transforms to stable β-Si_3N_4 at a higher temperature,[12] usually, in the presence of rare-earth oxide additives.[13,14] A third new high-pressure and high-temperature phase, c-Si_3N_4, which has a cubic-spinel structure, has been formed by using the laser-heating technique,[15] or by the shock-synthesized technique.[16] Due to important technological applications, an enormous effort is being made to obtain high pure Si_3N_4 whiskers or fibers. Generally, α- and β-Si_3N_4 whiskers are produced by three methods that are similar to those used to prepare SiC whiskers, that is, carbothermal reduction of silica, decomposition of imide compounds, and direct nitridation.[17–19] The α- and β-Si_3N_4 whiskers prepared by the above methods are usually in wide range of submicron ($\leq$ 1 μm) to ten microns in diameter. Very fine whiskers or fibers will cause environmental and health problems as do asbestos fibers.[19] If the whiskers with uniform micron-order diameter could be prepared, this would solve the problems in engineering applications. Recently, the newly distinct micro- and nanostructures with ribbon-shaped (belt-shaped) morphology in inorganic materials have received extensive attention in both fundamental research and technological applications.[20–24] Due to their brittleness, ceramic whiskers or fibers are regarded as materials of modest performance, especially under tension or bending conditions.[1] If ceramic whiskers or fibers with thin ribbon-shaped (belt-shaped) morphology can be achieved, it is expected that the new form, not only possesses more interesting mechanical properties, such as ductility or superplasticity of ceramic reinforcing composite materials, but also has novel optical properties.[1] In this article, we report on the growth of the thin, ribbon-shaped, micro-sized structurally uniform single crystals of α- and β-Si_3N_4 whiskers, which is achieved by ther-

[a] Dr. J. Hu, Dr. Y. Bando, Dr. Z. Liu, Dr. F. Xu, Dr. T. Sekiguchi, Dr. J. Zhan
Advanced Materials Laboratory and
Nanomaterials Laboratory, National Institute
for Materials Science (NIMS), Namiki 1–1, Tsukuba
Ibaraki 305–0044 (Japan)
Fax: (+81) 298-51-6280
E-mail: HU.Junqing@nims.go.jp

DOI: 10.1002/chem.200305390

mal-decomposition-nitridation of silicon monoxide (SiO) at high temperatures. The thin ribbons have uniform widths of ~2–3 microns, thicknesses of ~20–60 nm, and lengths that range from several hundreds of microns to the order of millimeters. The optical property (cathodoluminescence) was also investigated for the new ribbon-shaped form of this material.

Experimental Section

Uniform micro-sized α- and β-Si_3N_4 thin ribbons were grown in a vertical induction furnace. The induction furnace consists of a clear fused-quartz tube (50 cm in length, 12 cm in outer diameter and 0.25 cm in wall thickness), and an inductively-heated cylinder made of high-purity graphite (30 cm in length, 4.5 cm in outer diameter and 3.5 cm in inner diameter) coated with a C fiber thermo-insulating layer. The heated cylinder had one inlet and outlet C pipe on its top and bottom, respectively. A graphite crucible (3.0 cm in outer diameter, 3 mm in wall thickness, and 3 cm in height), that contained SiO powder (1.5 g, 99.99%, Sigma-Aldrich) was placed at the center cylinder zone.

After evacuation of the quartz tube to $\sim 2\times10^{-1}$ Torr, a pure N_2 flow was introduced through the tube at a flow rate of 1.0 L min^{-1}, and an ambient pressure in the tube. The crucible was rapidly heated and maintained at 1550 °C (measured by an optical pyrometer with an estimated accuracy of ±10 °C) for 1.5 h.

After the reaction was terminated and the furnace was cooled to the room temperature, the product was collected from the inner wall of the heated cylinder, and characterized by using an X-ray diffractometer (XRD, RINT 2200) with $Cu_{K\alpha}$ radiation, scanning electron microscopy (SEM, JSM-6700F) and transmission electron microscopy (TEM, JEM-3000F) attached with a parallel detection Gatan-666 electron energy loss spectrometer (EELS), and an X-ray energy dispersive spectrometer (EDS).

Cathodoluminescence (CL) spectroscopy was carried out by using a low energy CL (HRLE-CL) system, and a thermal-field-emission scanning electron microscopy (TFE-SEM, Hitachi S4200).

Results and Discussion

As-grown product was deposited (the yield of the product was estimated to be ~5%, according to the amount of SiO used) as pieces of gray-white wool-like material on the inner wall of the heated cylinder after the reaction was terminated. The XRD pattern of the product is shown in Figure 1.

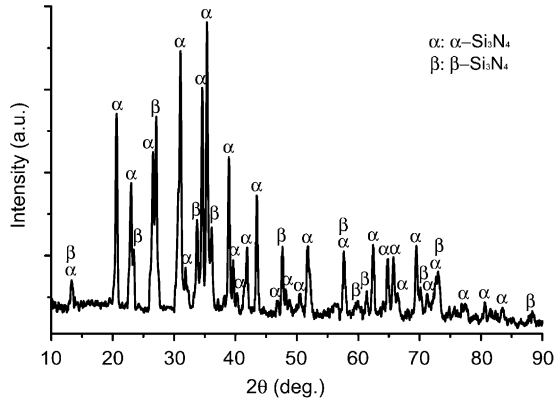

Figure 1. A XRD pattern recorded from the product grown by a high-temperature thermal-decomposition/nitridation route.

The peaks marked with α can be indexed as those from the hexagonal α-Si_3N_4 with lattice constants $a=7.750$ Å and $c=5.620$ Å, consistent with the standard values (JCPDS, 41–360, $a=7.754$ Å and $c=5.622$ Å) within experimental error; while the peaks indicated by β, can be identified as the hexagonal β-Si_3N_4 with lattice constants $a=7.588$ Å and $c=2.904$ Å, in accordance with the literature values (JCPDS, 33–1160, $a=7.604$ Å and $c=2.9075$ Å). Therefore, both α- and β- mixed phases of crystalline Si_3N_4 are obtained in the present route. No characteristic peaks from other impurities, such as Si, SiO, and SiC, are detected in the XRD pattern.

Examinations of SEM and TEM will shed light on the morphology characteristics of as-grown Si_3N_4 product. As seen from a low-magnification SEM image, the product consists of a large quantity of long and straight ribbon-shaped whiskers with a uniform micro-order diameter. Analysis of a number of the ribbons show that each has a diameter of around 2–3 microns, and a length of up to several hundreds of microns, some of them even have lengths in the order of millimeters. A high-magnification SEM image, Figure 2B,

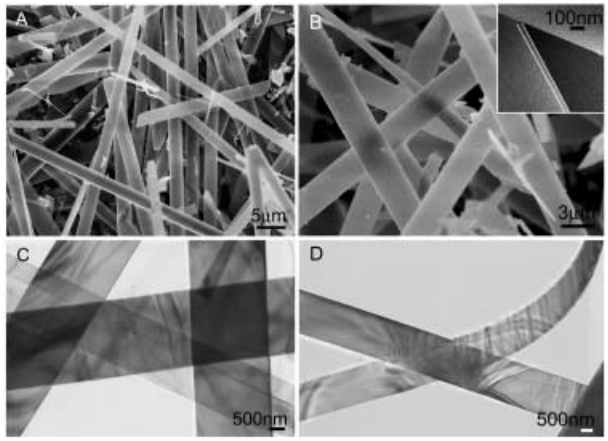

Figure 2. A) Low- and high-magnification. B) SEM images of as-grown straight uniform micro-sized α- and β-Si_3N_4 thin ribbons, respectively. An upper right inset (B) which shows the thickness of a ribbon imaged edged-on. TEM images of the uniform straight (C) and twisted (D) α- and β-Si_3N_4 thin ribbons, respectively.

further suggests that the product clearly displays a thin and wide uniform ribbon-shaped geometrical characteristic. The thickness of the ribbon can be deduced from the ribbons imaged edged-on, as shown in an upper right inset in Figure 2B, in which the thickness is indicated by two parallel lines. Careful examination of many ribbons with different lengths reveals that the thickness is estimated to be 20–60 nm. The TEM image in Figure 2C shows that the uniform ribbons are so thin that they are very transparent to the electron beam in the TEM imaging, even if three ribbons are overlapped. The TEM image in Figure 2D shows a twisted ribbon, in which many streaklike or ripple-type contrasts on the observed faces are due to the presence of strain, which originates from the lattice distortions in thin TEM samples;[23,25] this also suggests significant ductility and flexibility of the "advanced ceramic" Si_3N_4 ribbon-shaped whiskers.

High-resolution TEM (HRTEM) and electron diffraction (ED) studies will provide further insight into the microstructures of the new ribbon-shaped form for this material. Figure 3A shows a HRTEM image of one ribbon, in which the

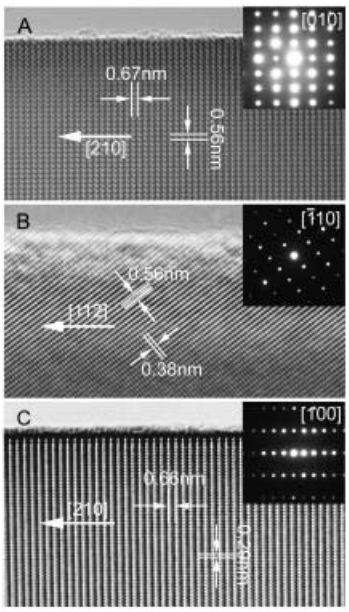

Figure 3. A) A HRTEM image of a α-Si_3N_4 ribbon with the [210] growth direction, an upper right inset showing its [010] zone axis ED pattern. B) A HRTEM image of a α-Si_3N_4 ribbon with the [112] growth direction, an upper right inset that shows the [−110] zone axis ED pattern. C) A HRTEM image of a β-Si_3N_4 ribbon with the [210] growth direction, an upper right inset showing the [100] zone axis ED pattern.

lattice fringes of the {100} and {001} have a *d*-spacing of 0.67 nm and 0.56 nm, respectively, for the hexagonal α-Si_3N_4, which can be clearly seen. The [210] crystallographic direction is parallel to the long axis direction of the ribbon, that is, the growth direction, which is perpendicular to the [001] crystallographic orientation of α-Si_3N_4. As seen from the image, this ribbon is a structurally-uniform single crystal, and no dislocations or other planar defects are observed within it. The edge of the ribbon is clean and very abrupt on an atomic scale, and there are no amorphous layers covering the surface. The corresponding ED pattern (an upper right inset) can be indexed as the [010] zone axis diffraction pattern of the α-Si_3N_4 single crystal. The out-of-focus diffraction pattern also suggests that long axis direction or the growth direction occurs along the [210] direction of the α-Si_3N_4 crystal. Careful HRTEM and ED examinations of this ribbon indicate that the structural uniformity of the single-crystal ribbon is perfectly maintained throughout the whole length. Figure 3B shows a HRTEM image of an other ribbon. The measured *d*-spacing of 0.56 nm and 0.38 nm are in agreement with those of the {001} and {110} crystallographic planes of α-Si_3N_4, respectively. The ED pattern, shown in the upper right inset, can be indexed as the [−110] zone axis diffraction pattern of the α-Si_3N_4 crystal. Similar HRTEM and ED studies reveal that this ribbon is also a structurally-uniform and defect-free single crystal, while the growth direction, different from the former, is demonstrated to be parallel to the [112] crystallographic orientation of the α-Si_3N_4 crystal. Figure 3C is a HRTEM image of another ribbon, in which the measured *d*-spacings of 0.66 nm and 0.29 nm are in accordance to the {100} and {001} crystallographic planes of the hexagonal β-Si_3N_4. The long axis direction or the growth direction of the ribbon is determined to be parallel to [210] crystallographic orientation of β-Si_3N_4, which is the same as one of the α-Si_3N_4 ribbons' growth direction. The corresponding ED pattern (lower right inset) can be indexed as the [100] zone axis diffraction pattern of the β-Si_3N_4 single crystal. In our experiment, examinations of several tens of these ribbons by HRTEM and ED methods suggest that these ribbons generally fall into the three types: A large part of the product (~60%) is α-Si_3N_4 ribbons in the [210] growth direction, as shown in Figure 3A, and another form with a small proportion is also α-Si_3N_4 ribbons with a different growth direction from the former, that is, the [112] direction, as shown in Figure 3B, the third type with considerable content is β-Si_3N_4 ribbons with the only [210] growth direction, as shown in Figure 3C.

The composition of individual Si_3N_4 ribbons has been characterized by using in-situ EDS and EELS analysis. The spectrum shown in Figure 4A reveals the presence of Si and

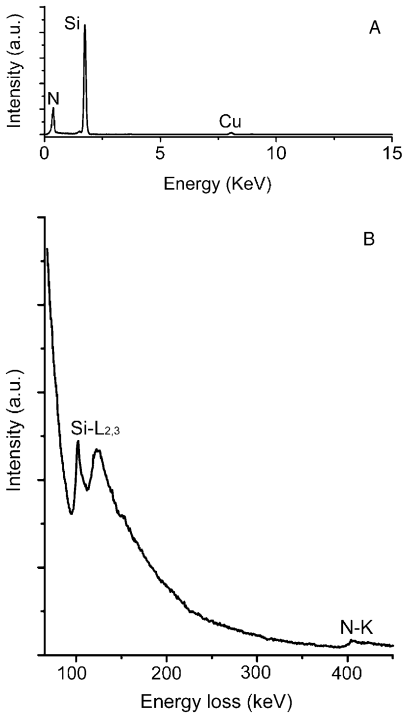

Figure 4. A) An EDS and B) an EEL spectrum, recorded from an Si_3N_4 ribbon.

N (a very weak Cu signal comes from a TEM grid) with the presence of no other impurities within a ribbon. Quantization of the spectrum gives the components (at. -%) of Si and N as ~42.4 and ~57.6 (calcd for Si_3N_4: Si, 42.85; N, 57.14), respectively; this outlines the stoichiometry of the Si_3N_4 ribbon. A representative EEL (Figure 4B) spectrum

(recorded by using a stationary focused 1 nm electron probe) also shows the composition of the α-Si_3N_4 ribbon. The peaks of the Si-$L_{2,3}$ edge (~99.3 eV) and N-K edge (~401.5 eV) indicate that the ribbon is composed of Si and N. No C K-shell ionization edge (~283.8 eV) can be seen in the spectrum, which indicates no C contamination from the crucible carbon material that was used. Quantization of the EEL spectrum shows the components of Si and N are close to that of the EDS analysis.

Cathodoluminescence was used to investigate the optical property of the new ribbon-shaped form of this material. Figure 5 shows a room temperature CL spectrum of these

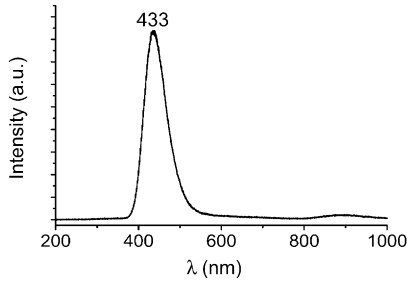

Figure 5. A room-temperature CL spectrum recorded from the α- and β-Si_3N_4 ribbons.

ribbons, which consists of one intensive blue emission peak at ~433 nm (~2.86 eV). Previous studies have defined defects in silicon nitride to be of four types, namely, Si–Si and N–N bonds, and Si and N dangling bonds.[26] Theoretical predictions have indicated that there are two nitrogen defect states that give rise to levels within the gap, namely N_4 and N_2^0, that are near the conduction and valence band, respectively.[27] According to this model, the strong peak at ~433 nm is due to recombination, either from the conduction band to the N_2^0 level, or from the valence band to the N_4 level.

It has been reported that the microribbons grown by a metal-catalyzed vapor-liquid-solid (VLS) process can be interpreted by a twin-plane growth mechanism,[28,29] in which a metal particle is located at the growth front of the ribbons, and acts as the catalytic active-site: the growth process of the ribbons was controlled by a twin-plane parallel to the flat surface of the microribbons. In our experiment, no catalytic metal was used, and no existence of twin-plane parallel to the flat surface of both α- and β-Si_3N_4 ribbons was observed in our TEM careful examination. Therefore, the growth of these ribbons may not be dominated by the above-proposed mechanism. In the present case, a Si vapor would be produced due to the thermal decomposition of SiO to $Si + SiO_2$.[30–33] Meanwhile, due to the high processing temperature, a carbothermal reduction of SiO and the crucible carbon material [SiO (g) + C (s) → Si (g) + CO (g)] may occur to some degree, and also help to produce a Si vapor. These Si vapors then react (nitride) with N_2 through a reaction, 3Si (vapor) + $2N_2$ (vapor) → Si_3N_4 (solid), at a suitable temperature region, and the formation of Si_3N_4 ribbons thus falls into a vapor-solid (VS) process.[34,35] In this reaction, some unstable gas intermediates such as SiN and Si_2N may be formed, which might play a role in the formation process for these ribbons. We named the process as a high-temperature thermal-decomposition-nitridation process. In this process, the reaction of as-formed Si vapors with N_2 will result in the formation Si_3N_4 nanoclusters (the nuclei of Si_3N_4 ribbons) on the inner wall of the heated cylinder. Some of these nanoclusters (or nuclei Si_3N_4 ribbons) have a low-surface energy among the crystal planes in both α- and β-Si_3N_4. These Si_3N_4 nanoclusters (or nuclei Si_3N_4 ribbons) are therefore energetically favorable, and serve as stable sites for the adhesion of additional Si_3N_4 molecules; this gives rise to the growth of the Si_3N_4 ribbons. Due to a high given temperature, the α-Si_3N_4 (metastable, low-temperature phase) will undergo phase transformation to stable β-Si_3N_4.[12] Usually, in the transformation of α- to β-Si_3N_4, rare-earth-oxide-assisted additions are required in order to initiate and enhance the transformation.[13,14] In our route, no earth-oxide phases are used, the transformation of α- to β-Si_3N_4 is believed to occur through a self-initiation process, and the transformation ratio is thus low, which is somewhat similar to that previously reported.[36] It is expected that by optimizing the reaction conditions, for example, by carefully selecting the deposition temperature, the pure-phase α-Si_3N_4 or β-Si_3N_4 ribbons can be produced by the present route. In most cases for both the α- and β-Si_3N_4 ribbons, their growths occur along the [210] direction. This fact can be simply explained by the "low energy" argument, that is, that the {1000} plane is one of the most densely-arranged planes in both α- and β-Si_3N_4,[18] and stacking along the [210] therefore becomes energetically favorable. The detailed growth mechanisms of the new ribbon-shaped form for Si_3N_4, however, are not fully understood, and require more systematic investigations.

Conclusion

In summary, this present work demonstrates that the structurally uniform micro-sized single crystals of α- and β-Si_3N_4 thin ribbons (or ribbon-shaped whiskers) can be grown by a high-temperature thermal-decomposition/nitridation route. The ribbons have uniform widths of ~2–3 microns, a thicknesses of ~20–60 nm, and lengths that range from several hundreds of microns to the order of millimeters. A room-temperature cathodoluminescence spectrum recorded from these ribbons shows one intensive blue emission peak at ~433 nm. The structurally-uniform ribbon-shaped single crystals of α- and β-Si_3N_4 whiskers with the above available sizes could make them useful as a specific reinforcement in "advanced ceramics", such as metal and ceramic matrix-composites, as well as perhaps an ideal structure with which to pin vortices in microelectronics for various applications as optical devices.

Acknowledgement

This work was supported by the Japan Society for the Promotion of Science (JSPS) Fellowship tenable at the National Institute for Materials Science, Tsukuba, (Japan).

[1] V. Valcárcel, A. Pérez, M. Cyrklaff, F. Guitián, *Adv. Mater.* **1998**, *10*, 1370.
[2] J. M. Garcés, A. Kuperman, D. M. Millar, M. M. Olken, A. J. Pyzik, W. Rafaniello, *Adv. Mater.* **2000**, *12*, 1725.
[3] H. G. Jeong, K. Hiraga, M. Mabuchi, K. Higashi, *Philos. Mag. Lett.* **1996**, *74*, 73.
[4] H. G. Jeong, K. Hiraga, M. Mabuchi, K. Higashi, *Acta. Mater.* **1998**, *46*, 6009.
[5] K. B. Lee, H. Kwon, *Metall. Mater. Trans.* A, **1999**, *30*, 2999.
[6] M. Mabuchi, K. Higashi, *Int. J. Plast.* **2001**, *17*, 399.
[7] N. Claussen, P. Beyer, R. Janssen, M. May, T. Selchert, J. F. Yang, T. Ohji, S. Kanzaki, A. Yamakawa, *Adv. Eng. Mater.* **2002**, *4*, 117.
[8] L. M. Peng, K. S. Han, J. W. Cao, K. Noda, *J. Mater. Sci. Lett.* **2002**, *21*, 279.
[9] S. V. Deshpande, E. Gulari, S. W. Brown, S. C. Rand, *J. Appl. Phys.* **1995**, *77*, 6534.
[10] A. R. Zanatta, L. A. O. Nunes, *Appl. Phys. Lett.* **1998**, *72*, 3127.
[11] F. Munakata, K. Mastsuo, K. Furuya, Y. Akimune, J. Ye, I. Ishikawa, *Appl. Phys. Lett.* **1999**, *74*, 3498.
[12] S. Shimada, T. Kataoka, *J. Am. Ceram. Soc.* **2001**, *84*, 2442.
[13] J. H. Dai, J. B. Li, Y. J. Chen, X. Z. Yang, *Phys. Status Solidi A*, **2003**, *198*, 91.
[14] H. Li, K. Komeya, J. Tatami, T. Meguro, Y. Chiba, M. Komatsu, *J. Ceram. Soc. Jpn.* **2001**, *109*, 342.
[15] A. Zerr, G. Miehe, G. Serghiou, M. Schwarz, E. Kroke, R. Riedel, H. Fueβ, P. Kroll, R. Boehler, *Nature* **1999**, *400*, 340.
[16] T. Sekine, T, Mitsuhashi, *Appl. Phys. Lett.* **2001**, 79, 2719.
[17] Y. Mizuhara, M. Noguchi, T. Ishihara, Y. Takita, *J. Am. Ceram. Soc.* **1995**, *78*, 109.
[18] Y. L. Li, Y. Liang, Z. Q. Hu, *J. Mater. Sci.* **1996**, *31*, 2677.
[19] S. Shimada, N. Akazawa, *J. Ceram. Soc. Jpn.* **1998**, *106*, 935.
[20] Z. W. Pan, Z. R. Dai, Z. L. Wang, *Science* **2001**, *291*, 1947.
[21] W. Shi, H. Peng, N. Wang, C. Li, L. Xu, C.-S. Lee, R. Kalish, S.-T. Lee, *J. Am. Chem. Soc.* **2001**, *123*, 11095.
[22] J. T. Sampanthar, H. C. Zeng, *J. Am. Chem. Soc.* **2002**, *124*, 6668.
[23] J. Q. Hu, X. L. Ma, N. G. Shang, Z. Y. Xie, N. B. Wong, C. S. Lee, S. T. Lee, *J. Phys. Chem.* **2002**, *106*, 3823.
[24] H. Q. Yan, R. R. He, J. Pham, P. D. Yang, *Adv. Mater.* **2003**, *15*, 402.
[25] Z. R. Dai, Z. W. Pan, Z. L. Wang, *J. Phys. Chem. B* **2002**, *106*, 1274.
[26] C. Savall, E. Bustarret, J. P. Stoquert, J. C. Bruyere, *Mater. Res. Soc. Symp. Proc.* **1993**, *284*, 77.
[27] S. V, Deshpande, E. Gulari, S. W. Brown, S. C. Rand, *J. Appl. Phys.* **1995**, *77*, 6534.
[28] R. S. Wagner, R. G. Treuting, *J. Appl. Phys.* **1961**, *32*, 2490.
[29] R. S. Wagner, W. C. Ellis, *Appl. Phys. Lett.* **1964**, *4*, 89.
[30] N. Wang, Y. H. Tang, Y. F. Zhang, C. S. Lee, S. T. Lee, *Phys. Rev. B* **1998**, *58*, 16024.
[31] S. T. Lee, Y. F. Zhang, N. Wang, Y. H. Tang, I. Bello, C. S. Lee, *J. Mater. Res.* **1999**, *14*, 4503.
[32] W. S. Shi, H. Y. Peng, L. Xu, N. Wang, Y. H. Tang, S. T. Lee, *Adv. Mater.* **2000**, *12*, 1927.
[33] J. L. Gole, J. D. Stout, W. L. Rauch, Z. L. Wang, *Appl. Phys. Lett.* **2000**, *76*, 2346.
[34] G. W. Sears, *Acta Metall.* **1956**, *3*, 268.
[35] P. D. Yang, C. M. Lieber, *J. Mater. Res.* **1997**, *12*, 2981.
[36] K. B. Tang, J. Q. Hu, Q. Y. Lu, Y. Xie, J. S. Zhu, Y. T. Qian, *Adv. Mater.* **1999**, *11*, 653.

Received: July 26, 2003 [F5390]